

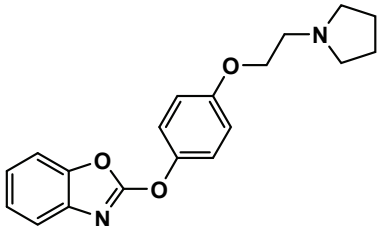
SUPPLEMENTARY MATERIAL TO
**Design of benzimidazoles, benzoxazoles, benzothiazoles and
thiazolopyridines as leukotriene A₄ hydrolase inhibitors through
3D-QSAR, docking and molecular dynamics**

MARCOS LORCA¹, MARIO FAÚNDEZ², C. DAVID PESSOA-MAHANA², GONZALO RECABARREN-GAJARDO^{2,3}, BENJAMIN DIETHELM-VARELA², DANIELA MILLÁN⁴, ISMAIL CELIK⁵, MARCO MELLADO⁶, ILEANA ARAQUE¹, JAIME MELLA^{1,7*} and JAVIER ROMERO-PARRA^{8**}

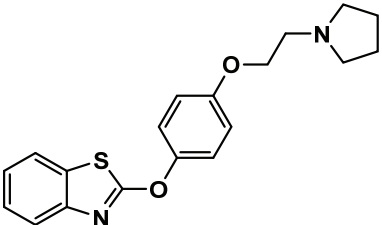
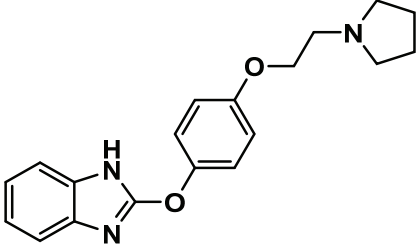
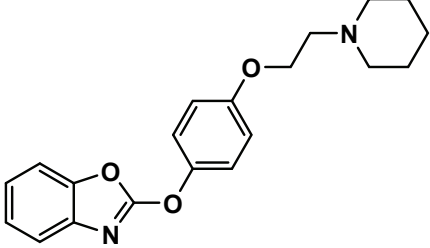
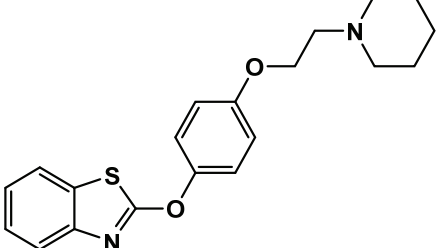
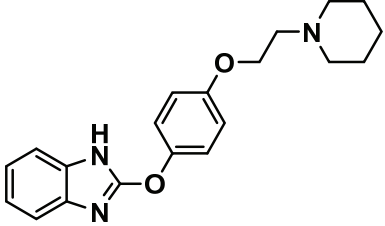
¹*Institute of Chemistry and Biochemistry, Faculty of Science, University of Valparaíso, Valparaíso 2360102, Chile,* ²*Faculty of Chemistry and Pharmacy, Pontifical Catholic University of Chile, Santiago 7820436, Chile,* ³*Interdisciplinary Center for Neurosciences, Pontifical Catholic University of Chile, Santiago 8330024, Chile,* ⁴*Integrative Center for Biology and Applied Chemistry, Bernardo O'Higgins University, Santiago 8370854, Chile,* ⁵*Department of Pharmaceutical Chemistry, Faculty of Pharmacy, Erciyes University, Kayseri 38039, Turkey,* ⁶*Instituto de Investigación y Postgrado, Facultad de Ciencias de la Salud, Universidad Central de Chile, Santiago 8330507, Chile,* ⁷*Chilean Pharmacopeia Research Center, University of Valparaíso, Valparaíso 2360134, Chile and* ⁸*Department of Organic Chemistry and Physical Chemistry, Faculty of Chemistry and Pharmaceutical Sciences, University of Chile, Santiago 8380544, Chile*

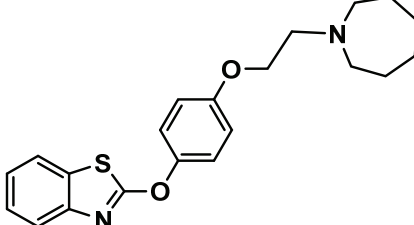
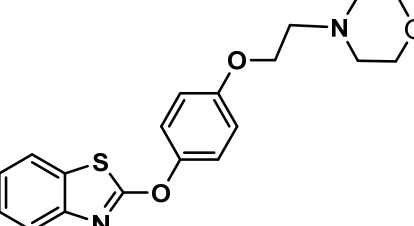
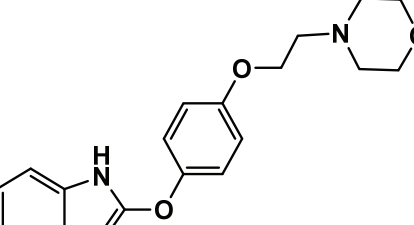
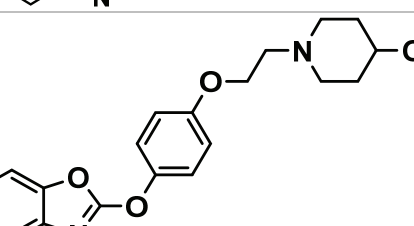
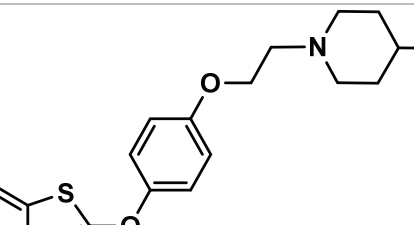
J. Serb. Chem. Soc. 88 (1) (2023) 25–39

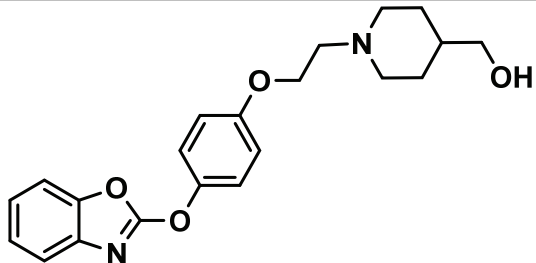
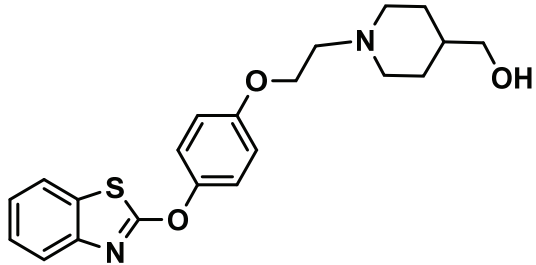
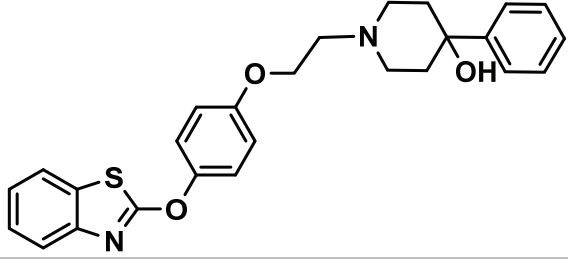
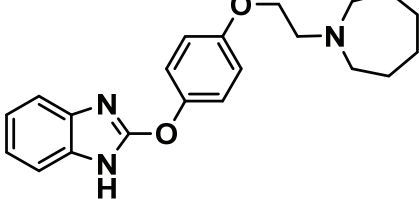
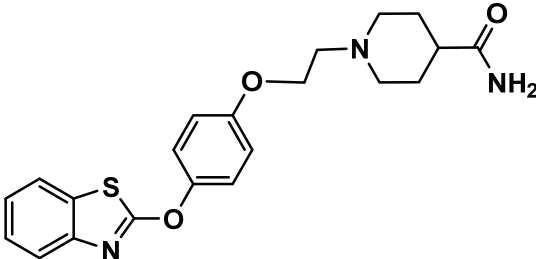
Table S-I. Chemical structure and pIC_{50} values of the studied LTA₄H inhibitors

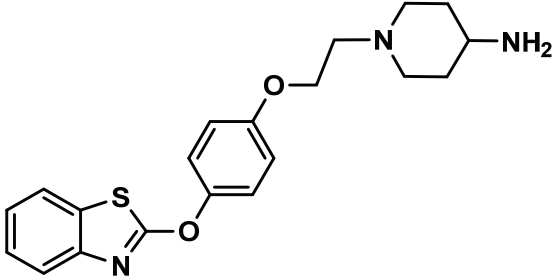
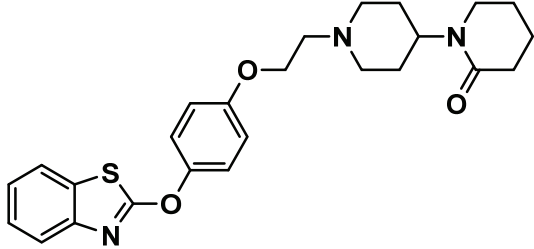
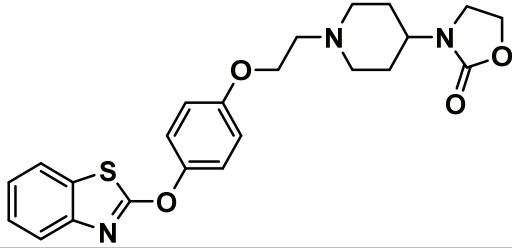
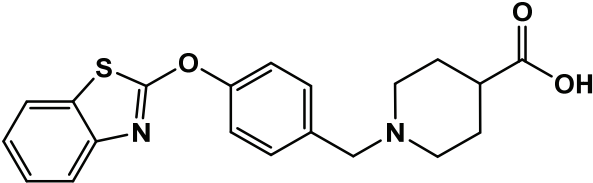
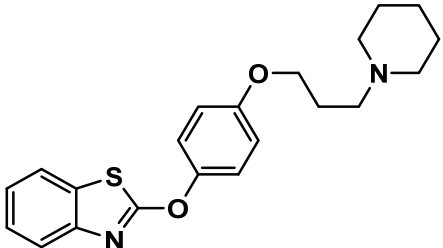
N°	Structure	IC ₅₀ / nM	pIC ₅₀
1		7	8.155

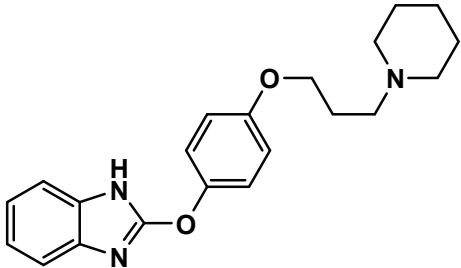
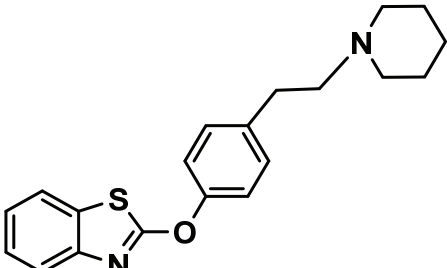
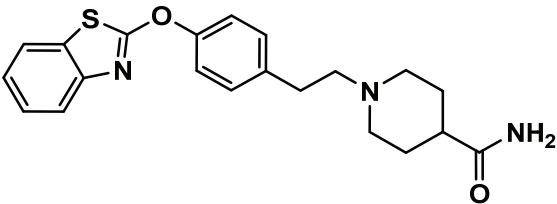
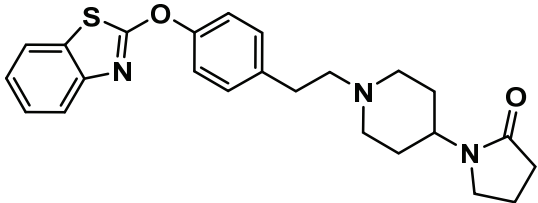
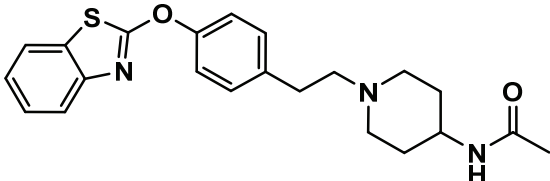
* Corresponding authors. E-mail: (*)jaime.mella@uv.cl; (**)javier.romero@ciq.uchile.cl

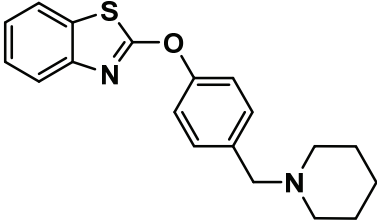
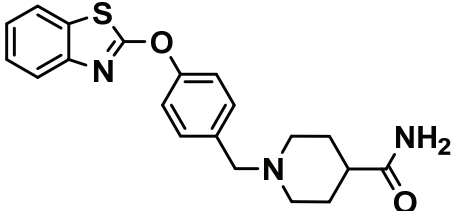
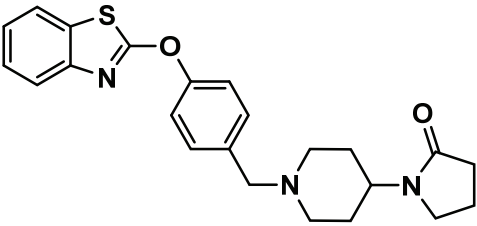
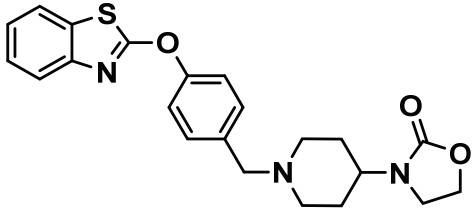
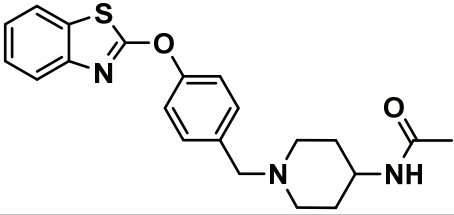
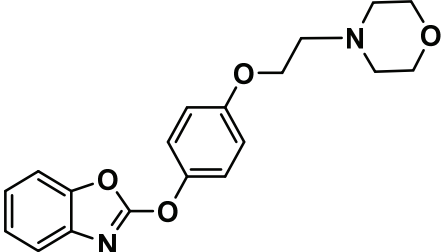
N°	Structure	IC_{50} / nM	pIC_{50}
2		14	7.854
3		84	7.076
4		11	7.959
5		54	7.268
6		110	6.959

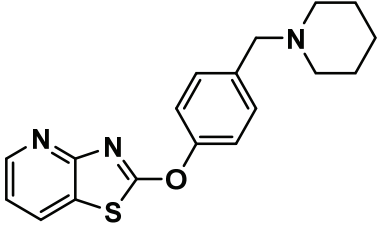
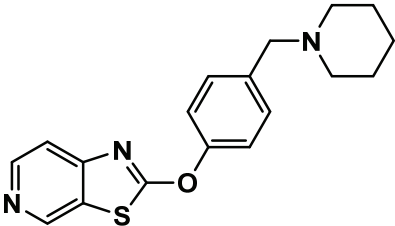
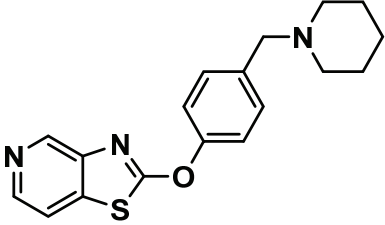
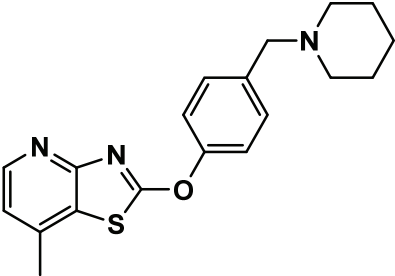
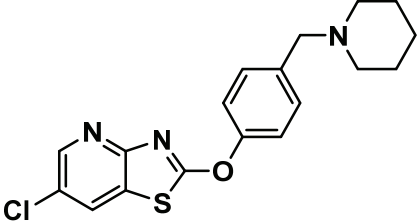
N°	Structure	IC ₅₀ / nM	pIC ₅₀
7		66	7.180
8		350	6.456
9		3000	5.523
10		9	8.046
11		31	7.509

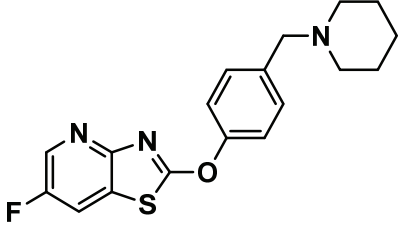
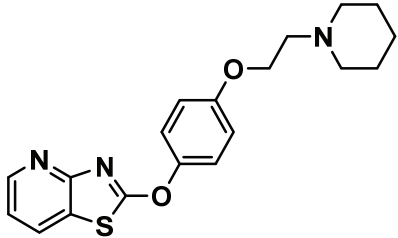
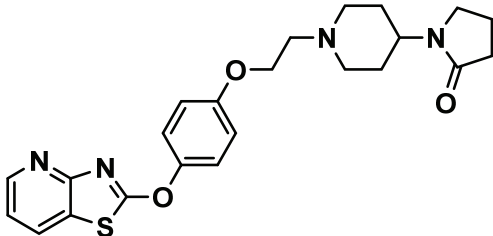
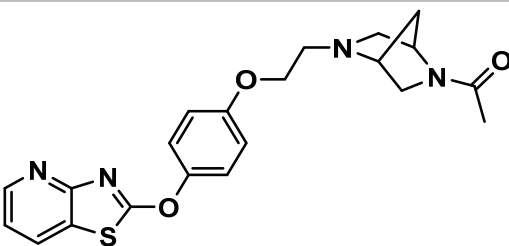
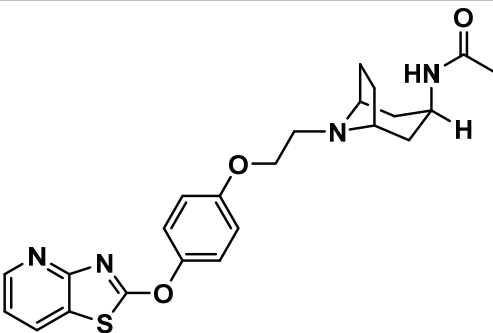
N°	Structure	IC_{50} / nM	pIC_{50}
12		14	7.854
13		13	7.886
14		66	7.180
15		140	6.584
16		13	7.886

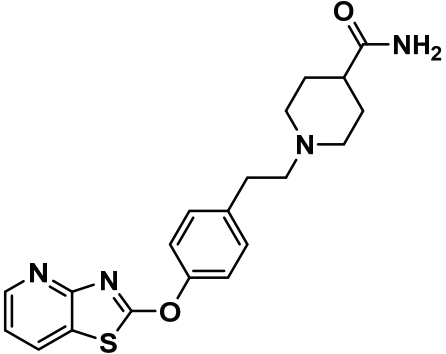
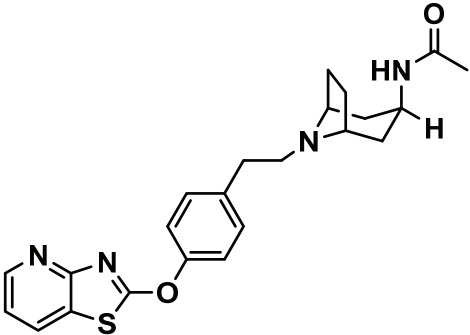
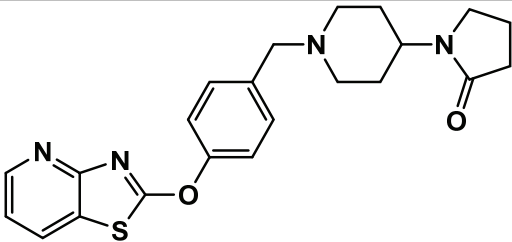
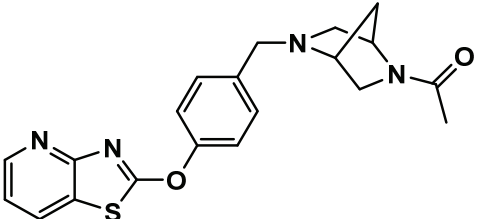
N°	Structure	IC ₅₀ / nM	pIC ₅₀
17		66	7.180
18		70	7.155
19		11	7.959
20		11	7.959
21		87	7.060

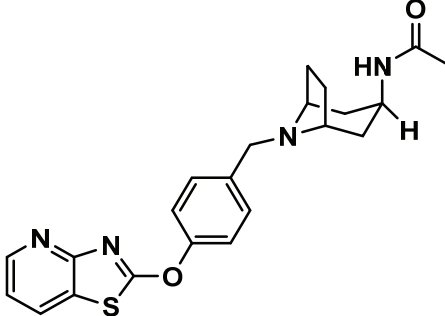
N°	Structure	IC_{50} / nM	pIC_{50}
22		140	6.854
23		17	7.770
24		28	7.553
25		13	7.886
26		35	7.456

N°	Structure	IC ₅₀ / nM	pIC ₅₀
27		59	7.229
28		17	7.770
29		12	7.921
30		10	8.000
31		12	7.921
32		58	7.237

N°	Structure	IC_{50} / nM	pIC_{50}
33		3	8.523
34		614	6.212
35		1800	5.745
36		33	7.481
37		40	7.398

N°	Structure	IC ₅₀ / nM	pIC ₅₀
38		29	7.538
39		8	8.097
40		6	8.222
41		7	8.155
42		4	8.398

N°	Structure	IC_{50} / nM	pIC_{50}
43		11	7.959
44		0.3	9.523
45		6	8.222
46		5	8.301

N°	Structure	IC_{50} / nM	pIC_{50}
47		1	9.000

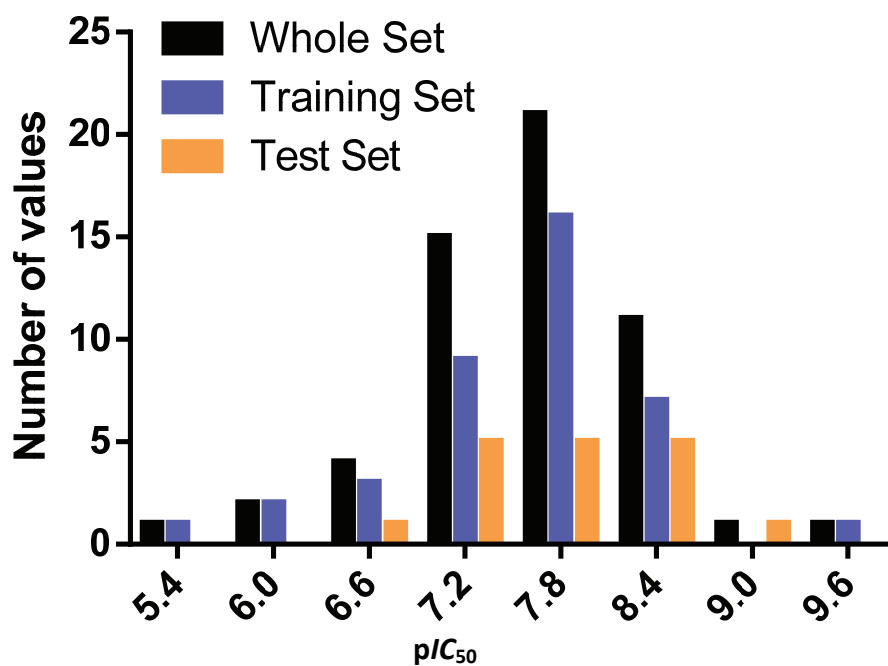


Fig. S-1. Histogram of frequency data portraying a uniform distribution of the pIC_{50} values of every inhibitory heterocyclic compound. Blue columns represent the training set molecules, orange columns represent the test set molecules and black columns represent the complete set molecules.

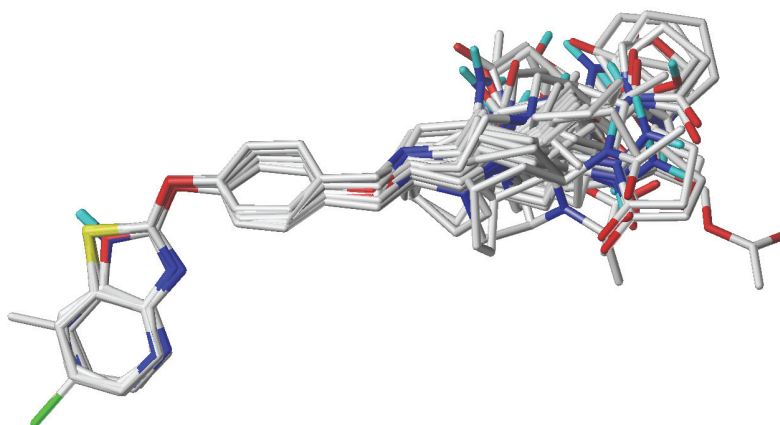


Fig. S-2. Superimposed structures of all compounds used in CoMFA/CoMSIA models.

Docking supplementary information

After the CoMFA and CoMSIA models were successfully built, 10 molecules (**1x–10x**) were designed as proposed inhibition compounds and tested with both models to obtain the new predicted pIC_{50} values. Subsequently, the docking assays of the compounds **9**, **44** and **1x–10x** were performed over the human LTA₄H (PDB_{ID}: 3FTS).¹ LTA₄H is made up of three distinctive domains, namely, *N*-terminal (residues 1–207), catalytic domain (residues 208–450), and *C*-terminal (residues 461–610).^{2,3} The catalytic binding pocket is located at the interface of these domains, mostly towards the catalytic domain. Whereas the *N*-terminal is completely composed of long-stranded β -sheets, the other two domains are made of α -helices. The metal ion-binding site is formed by amino acid residues only from the catalytic domain such as His295, His299 and of Glu318.² The grid where **9**, **44** and the proposed compounds **1x–10x** were docked was established based on the putative amino acids of the catalytic site, such as Arg563, Lys565 and Tyr383,^{2,4-6} with the zinc atom as the centre of the grid in order to obtain the binding mode of every compound and the docking descriptors.

Compounds **9** and **44** were chosen to be docked since they were the least and the most active LTA₄H inhibitors of the reported studied series, respectively. Therefore, to validate our docking assays, we compared the binding energies of the inhibitors **9** and **44** given by our docking experiments with their reported IC_{50} values. Results showed that the compound **9**, which has the highest IC_{50} value (3000 nM), displayed a deficient binding energy of -32.17 kJ/mol, which would explain the lower ability of **9** to inhibit the enzyme compared to the other molecules in table 1. Likewise, the most active inhibitory compound, the derivative **44**, had the lowest IC_{50} value (0.3 nM) and displayed an efficient binding energy of -43.14 kJ/mol, demonstrating a good correlation between the

experimental evidence and the theoretical information by our docking assays. Besides, the proposed compounds **1x–10x** also displayed efficient binding energies when they were docked into the catalytic site of the enzyme. Indeed, their values are comparable to the most active inhibitory compound (**44**).

The most active inhibitor **44** and the least active inhibitor **9** showed similar types of interactions but they were not exactly the same. Compound **44** formed a hydrogen bond interaction with Glu384, while compound **9** formed a hydrogen bond with Lys565. These different interactions could explain their different IC₅₀ values and their different binding energies. Pharmacological compounds or inhibitors could exhibit multiple binding modes and contribute similarly to the overall affinity,⁷ but when ligands are a part of a same chemical family, they often exhibit different sorts of affinity, potency, or pharmacological response, even if they settle into a biological target in a similar manner and performed similar interactions.⁸

Molecular docking of the compounds **9**, **44** (Fig. S-3), **1x**, **3x–6x**, **9x** and **10x** showed that all these derivatives are arranged in the same manner into the catalytic site of the LTA₄H enzyme, and all their thiazolopyridine rings overlap, that is to say the sulphur and nitrogen atoms at position 1- and 3- coincided, respectively (Fig. S-3). The compounds **9**, **44**, **1x**, **3x–6x** exhibited a hydrogen bond interaction with Tyr378 through the nitrogen atom at position 3- of their thiazolopyridine rings. The compounds **2x**, **7x** and **8x** were also arranged in the same manner as the other derivatives designed and shown in table 5, that is with their thiazolopyridine rings overlapping at the same direction within the catalytic site. Nonetheless, there is no coincidence of **2x**, **7x** and **8x** between the sulphur and nitrogen atoms with respect to the compounds **9**, **44**, **1x**, **3x–6x**, **9x** and **10x**, with these atoms being in opposite positions (Fig. S-3). The fact that the thiazolopyridine rings of the derivatives **2x**, **7x** and **8x** were inverted led to the loss of the hydrogen bond interaction between the amino acid Tyr378 and the nitrogen atom at position 3- of the heterocycles. Notwithstanding, the lack of this hydrogen bond interaction is balanced by the formation of a π - π interaction in **2x**, **7x** and **8x** between the pyridine rings of thiazolopyridines and the Tyr383 residue of the enzyme (Fig. S-3).

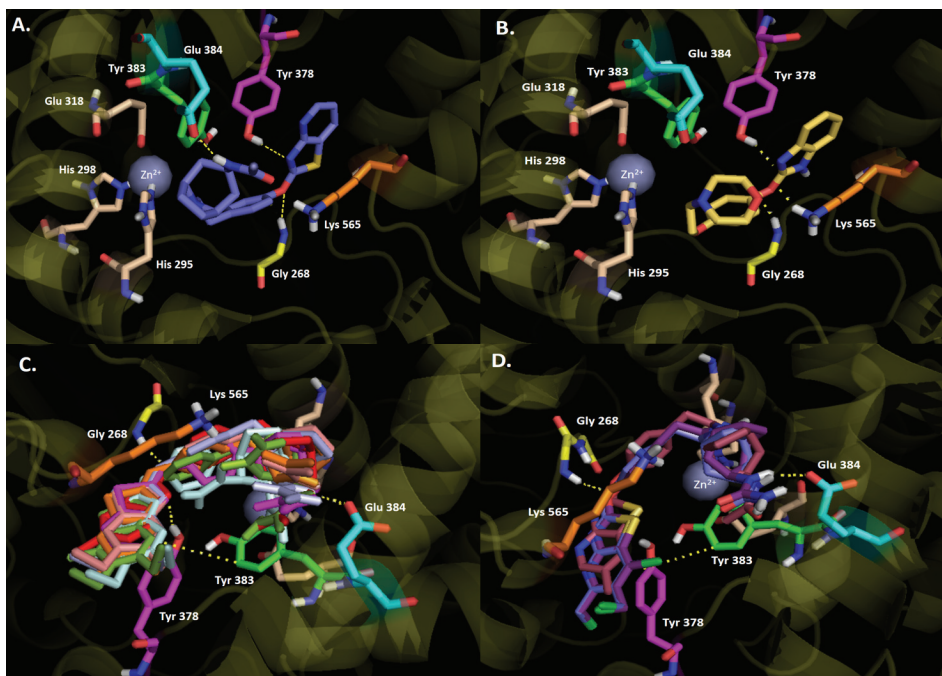


Fig. S-3. Predicted binding mode and predicted intermolecular interactions among **44**, **9**, **1x–10x** and the residues of the catalytic site of human LTA₄H. A. Compound **44** (most active inhibitor; H-bonding with Gly268, Tyr378 and Glu384). B. Compound **9** (least active inhibitor; H-bonding with Gly268, Tyr378 and Lys 565). C. Compounds **1x**, **3x–6x**, **9x** and **10x** (H-bonding with Gly268, Tyr378, Glu384 and Lys565 for **9x** and **10x**; π - π interaction with Tyr383 for **9x** and **10x**). D. Compounds **2x**, **7x** and **8x** (H-bonding with Gly268 and Glu384; π - π interaction with Tyr383)

All docked derivatives were shown to carry out a hydrogen bond interaction with Gly268 and Glu384 (except **10x**). The first one occurs due the oxygen atom between the phenyl rings and the thiazolopyridines, and the second one occurs through the hydrogen atoms of the amides or ureic groups placed at position 4- of the azabicyclooctane rings that all molecules contain (Fig. S-3).

The proposed compounds **9x** and **10x** did not perform a hydrogen bond interaction with Tyr378 (like the analogues **9**, **44**, **1x**, **3x–6x**), because their thiazolopyridine frameworks are slightly inclined to disfavoring the formation of this interaction. Notwithstanding, these molecules showed a π - π interaction through the amino acid Tyr383 and the pyridine rings of their thiazolopyridines. In addition, these molecules possess a second amide group at the azabicyclooctane core, which carried out an extra hydrogen bond interaction between the oxygen atom of the carbonyl group of the second amide and Lys565 residue. Therefore, these two different interactions could balance the lack of a hydrogen bond with Tyr378. Indeed, in the case of the hydrogen bond interaction

with Lys565, our CoMFA-steric contour map and CoMSIA-hydrogen bond acceptor contour map have demonstrated that the inclusion of an extra amide group in **9x** and **10x** led to a better inhibitory activity over the enzyme.

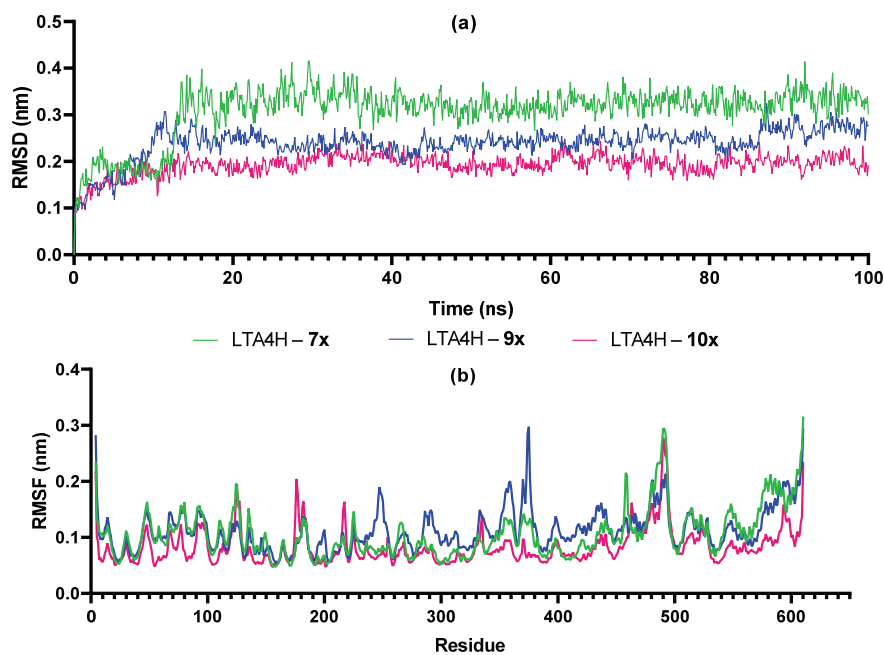


Fig. S-4. Trajectory analysis of molecular dynamics simulation of leukotriene A₄ hydrolase (LTA₄H) and compounds **7x**, **9x** and **10x**. (a) RMSD of compound LTA₄H – **7x**, LTA₄H – **9x** and LTA₄H – **10x** complexes, (b) RMS fluctuation values during the period of 100 ns simulation

REFERENCES

1. D. R. Davies, B. Mamat, O. T. Magnusson, J. Christensen, M. H. Haraldsson, R. Mishra, B. Pease, E. Hansen, J. Singh, D. Zembower, H. Kim, A. S. Kiselyov, A. B. Burgin, M. E. Gurney, L. J. Stewart, *J. Med. Chem.* **52** (2009) 4694 (<https://doi.org/10.1021/jm900259h>)
2. M. M. Thunnissen, P. Nordlund, J. Z. Haeggström, *Nat. Struct. Biol.* **8** (2001) 131 (<https://doi.org/10.1038/84117>)
3. A. Rinaldo-Matthis, J.Z. Haeggstrom, *Biochimie* **92** (2010) 676 (<https://doi.org/10.1016/j.biochi.2010.01.010>)
4. P. C. Rudberg, F. Tholander, M. Andberg, M. M. Thunnissen, J. Z. Haeggström, *J. Biol. Chem.* **279** (2004) 27376 (<https://doi.org/10.1074/jbc.M401031200>)
5. R. J. Snelgrove, *Thorax* **66** (2011) 550 (<https://doi.org/10.1136/thorajxnl-2011-200234>)
6. A. Wetterholm, J. F. Medina, O. Rådmark, R. Shapiro, J. Z. Haeggström, B. L. Vallee, B. Samuelsson, *Proc. Natl. Acad. Sci. U. S. A.* **89** (1992) 9141 (<https://doi.org/10.1073/pnas.89.19.9141>)

7. E. Stjernschantz, C. Oostenbrink, *Biophys. J.* **98**, (2010) 2682
(<https://doi.org/10.1016/j.bpj.2010.02.034>)
8. G. J. Kersh, E. N. Kersh, D. H. Fremont, P. M. Allen, *Immunity* **9** (1998) 817
([https://doi.org/10.1016/S1074-7613\(00\)80647-0](https://doi.org/10.1016/S1074-7613(00)80647-0)).